Science of the Total Environment 876 (2023) 162729

Contents lists available at ScienceDirect

Science of the Total Environment

journal homepage: www.elsevier.com/locate/scitotenv

Assessing the photodegradation potential of compounds derived from the photoinduced weathering of polystyrene in water

Debora Fabbri [a], Luca Carena [a], Debora Bertone [a], Marcello Brigante [b], Monica Passananti [a,c,*], Davide Vione [a,**]

[a] Dipartimento di Chimica, Università di Torino, Via Pietro Giuria 5, 10125 Torino, Italy
[b] Université Clermont Auvergne, CNRS, INP Clermont Auvergne, Institut de Chimie de Clermont-Ferrand, F-63000 Clermont-Ferrand, France
[c] Institute for Atmospheric and Earth System Research/Physics, Faculty of Science, University of Helsinki, FI-00014 Helsinki, Finland

HIGHLIGHTS

- Both benzoate and acetophenone undergo important reactions with $^{\bullet}OH$.
- Acetophenone is also degraded by $CO_3^{\bullet-}$, while its direct photolysis would be minor.
- Volatilisation would be an important removal pathway for aqueous acetophenone.
- Both compounds show limited reactivity with $Br_2^{\bullet-}$.
- Both compounds have higher stability in high-DOC freshwaters and in seawater.

GRAPHICAL ABSTRACT

Benzoate and acetophenone derive from polystyrene photodegradation and are in turn photodegraded in natural surface waters.

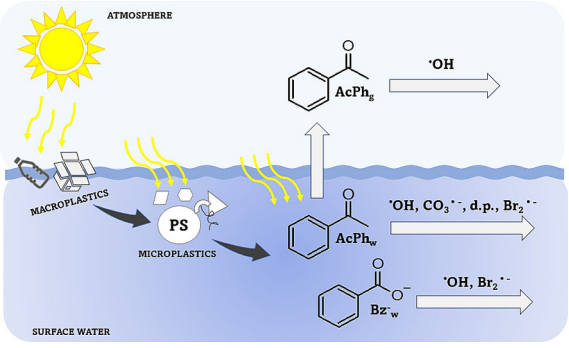

ARTICLE INFO

Editor: Dimitra A Lambropoulou

Keywords:
Environmental photochemistry
Photochemical fate
Kinetic constant
Polystyrene
Aromatic compounds
Natural waters

ABSTRACT

Benzoate (Bz^-) and acetophenone (AcPh) are aromatic compounds known to be produced by sunlight irradiation of polystyrene aqueous suspensions. Here we show that these molecules could react with $^{\bullet}OH$ (Bz^-) and $^{\bullet}OH$ + $CO_3^{\bullet-}$ (AcPh) in sunlit natural waters, while other photochemical processes (direct photolysis and reaction with singlet oxygen, or with the excited triplet states of chromophoric dissolved organic matter) are unlikely to be important. Steady-state irradiation experiments were carried out using lamps, and the time evolution of the two substrates was monitored by liquid chromatography. Photodegradation kinetics in environmental waters were assessed by a photochemical model (APEX: Aqueous Photochemistry of Environmentally-occurring Xenobiotics). In the case of AcPh, a competitive process to aqueous-phase photodegradation would be volatilisation followed by reaction with gas-phase $^{\bullet}OH$. As far as Bz^- is concerned, elevated dissolved organic carbon (DOC) levels could be important in protecting this compound from aqueous-phase photodegradation. Limited reactivity of the studied compounds with the dibromide radical ($Br_2^{\bullet-}$, studied by laser flash photolysis) suggests that $^{\bullet}OH$ scavenging by bromide, which yields $Br_2^{\bullet-}$, would be poorly offset by $Br_2^{\bullet-}$-induced degradation. Therefore, photodegradation kinetics of Bz^- and AcPh should be slower in seawater (containing $[Br^-] \sim 1$ mM) compared to freshwaters. The present findings suggest that photochemistry would play an important role in both formation and degradation of water-soluble organic compounds produced by weathering of plastic particles.

* Correspondence to: M. Passananti, Institute for Atmospheric and Earth System Research/Physics, Faculty of Science, University of Helsinki, FI-00014 Helsinki, Finland.
** Corresponding author.
E-mail addresses: monica.passananti@helsinki.fi (M. Passananti), davide.vione@unito.it (D. Vione).

http://dx.doi.org/10.1016/j.scitotenv.2023.162729
Received 19 December 2022; Received in revised form 21 February 2023; Accepted 5 March 2023
Available online 10 March 2023

1. Introduction

Pollution by plastics is a growing environmental concern, especially for natural waters where plastic inputs have reached alarming proportions. It has been calculated that approximately 6300 Mt of plastic waste had been produced until 2015 and around 79 % (~ 4977 Mt) was accumulated in landfills or the natural environment (Geyer et al., 2017). The majority of plastic debris reaches the sea through rivers, and different estimates have been performed to quantify the amount of plastic transported by rivers to the sea. Such estimates range from 0.47 up to 12.7 million metric tons of plastic per year (Jambeck et al., 2015; Schmidt et al., 2017).

Once they reach the natural environment, plastics undergo weathering largely due to the action of sunlight that operates through two main processes. The former is sunlight-induced fragmentation of plastic objects (macroplastics) into smaller particles, *i.e.*, micro- and finally nanoplastics (Andrady et al., 2022). Microplastics have been defined as plastic particles in the 1–5000 μm size range, while nanoplastics are smaller than 1 μm (Frias and Nash, 2019). Adding to the primary environmental sources of small plastic particles (which include their use in fertilizers and release upon runoff from artificial turf pitches; Kumar et al., 2020; Salthammer, 2022), fragmentation highly affects environmental behaviour because of the reactivity of small-sized plastics (Bianco et al., 2020). These can impact living organisms to a different degree than macroplastics, for instance by reaching tissues and crossing membranes (Liu et al., 2021). The second weathering process by sunlight is photodissolution, which consists in photoinduced release to the water phase of additives or polymer fragmentation products (Gewert et al., 2015; Zhu et al., 2020). The chemical compounds arising from plastic weathering can have adverse effects on living organisms, in particular if they have endocrine-disruption properties (Burgos-Aceves et al., 2021). These compounds might also play potential role as markers of plastic pollution, especially in cases where plastics are difficult to detect, *e.g.*, because of their small size: nanoplastics are particularly challenging as far as detection and polymer identification are concerned (Jakubowicz et al., 2021).

The environmental role of plastic weathering products is deeply affected by environmental persistence. For instance, a persistent compound can undergo accumulation up to relatively high concentration values, which enhances its effects and makes quantification much easier. However, because of its persistence, it can also be transported quite far from the pollution source.

Sunlight, in addition to being a major driver of plastic weathering, would also play a role in the transformation of plastic degradation products in natural surface waters. In particular, solar radiation would operate through direct photolysis and indirect photochemistry (Guo et al., 2023). Direct photolysis occurs when a compound absorbs sunlight and the absorption process triggers transformation by, for instance, ionisation, bond breaking, and excited-state reactivity (Katagi, 2018). In the case of indirect photochemistry, sunlight is absorbed by naturally occurring photosensitisers such as nitrate, nitrite, and chromophoric dissolved organic matter (CDOM). These species absorb sunlight and yield the so-called photochemically produced reactive intermediates (PPRIs), of which the main ones are the hydroxyl ($^{\bullet}OH$) and carbonate ($CO_3^{\bullet-}$) radicals, singlet oxygen ($^1O_2$), and CDOM triplet states ($^3CDOM^*$) (Yan and Song, 2014; Vione and Scozzaro, 2019). The photolysis of nitrate and nitrite yields $^{\bullet}OH$, while CDOM irradiation yields $^3CDOM^*$, $^1O_2$, and $^{\bullet}OH$. $CO_3^{\bullet-}$ is produced upon oxidation of HCO_3^-/CO_3^{2-} by $^{\bullet}OH$, or CO_3^{2-} oxidation by $^3CDOM^*$ (Rosario-Ortiz and Canonica, 2016; McNeill and Canonica, 2016; Yan et al., 2019). The PPRIs have very low steady-state concentrations in sunlit natural waters (10^{-18}–10^{-14} M), because they are quickly scavenged/quenched by several processes. In particular: $^{\bullet}OH$ is mainly scavenged by dissolved organic matter (DOM, either chromophoric or not) and, usually to a lesser extent, by HCO_3^-/CO_3^{2-}; $CO_3^{\bullet-}$ is mostly scavenged by DOM; $^3CDOM^*$ is mainly quenched by O_2 to produce $^1O_2$, with ~50 % yield; finally, $^1O_2$ is mostly quenched by collision with water (Gligorovski et al., 2015; Yan et al., 2019; Ossola et al., 2021). In the case of saltwater and especially seawater, the main scavenging process for $^{\bullet}OH$ is the reaction with Br^- to eventually yield $Br_2^{\bullet-}$, which is also a PPRI (Parker and Mitch, 2016). The budget between photoproduction and scavenging/quenching controls PPRIs occurrence in natural waters under sunlight. In particular, $^{\bullet}OH$ and $CO_3^{\bullet-}$ tend to be more concentrated at low values of the dissolved organic carbon (DOC), while the opposite happens in the case of $^3CDOM^*$ and $^1O_2$ (Vione and Scozzaro, 2019). The higher is the steady-state concentration of a PPRI, the higher is its ability to trigger transformation of dissolved compounds, including those released by plastic weathering.

Previous studies have shown that weathering of polystyrene particles under sunlight yields a number of dissolved compounds, among which benzoate (Bz^-) and acetophenone (AcPh) have been identified as important photoproducts (Bianco et al., 2020) that can also undergo further degradation. It is possible that photoinduced production of reactive species by polystyrene itself contributes to the weathering process (Ding et al., 2022). For Bz^- and AcPh, reactivity with $^{\bullet}OH$ and $CO_3^{\bullet-}$ can be assessed on the basis of the literature (Buxton et al., 1988; Neta et al., 1988; Wols and Hofman-Caris, 2012), but no data are currently available for the other photoinduced reactions. Therefore, the goal of this work is to assess the potential for abiotic degradation of both compounds by direct and indirect photochemistry, with the purpose of better defining their fate in the environment. In the case of semivolatile AcPh, we also consider its potential partitioning between the liquid and the gas phase and, finally, its possible photodegradation in both surface waters and the atmosphere. The reactivity of Bz^- and AcPh with $Br_2^{\bullet-}$ was also investigated, to tentatively assess photodegradation of the two compounds in seawater *vs.* freshwater.

2. Materials and methods

2.1. Chemicals

All reagents, solvents, and eluents were of analytical grade, or gradient-grade for liquid chromatography. They were purchased from: Sigma-Aldrich (4-carboxybenzophenone, sodium benzoate, acetophenone, 2-nitrobenzaldehyde, furfuryl alcohol, H_2O_2, $NaNO_3$, and NaBr); Alfa Aesar (Rose Bengal and NaOH), and VWR International (acetonitrile, methanol, and H_3PO_4). The mentioned chemicals were used as received, without further purification. Water was produced by a Milli-Q apparatus (Millipore, resistivity 18.2 MΩ cm, TOC = 0.2 ppm).

2.2. Irradiation experiments

Solutions to be irradiated (5 mL total volume) were placed in cylindrical Pyrex glass cells (height 2.5 cm, diameter 4.0 cm, cut-off wavelength 280 nm), equipped with a lateral neck for liquid insertion and withdrawal. The neck was tightly closed with a screw cap during the irradiation experiments, which took place under magnetic stirring. Irradiation sources in different experiments were a UVB lamp (Philips Narrowband TL20W/01 RS, emission maximum at 313 nm), a UVA lamp (black lamp TL-D 16 W BLB, emission maximum at 369 nm), or a yellow lamp (TL-D 18 W/16, emission maximum at 580 nm). These lamps produce a limited amount of heating in the irradiated solutions, the temperature of which was around 30 °C. Three cells were simultaneously irradiated under the same lamp, in positions that ensured a limited degree of variability in lamp irradiance (±5 %, checked with a Testo® 540 lx-meter, as compared to typical ~10 % reproducibility of irradiation experiments).

The UVB lamp was used to study the direct photolysis of Bz^- and AcPh, which both show an absorption tail with some absorbance in the UVB region and very low UVA absorbance. The UVA lamp was used to achieve selective excitation of 4-carboxybenzophenone (CBBP), which was employed as CDOM proxy to study the reactions with $^3CDOM^*$. Because previous studies have shown that $^3CBBP^*$ has comparable reactivity as average $^3CDOM^*$ (Carena et al., 2019), CBBP irradiation can be used to assess the second-order reaction rate constants between dissolved compounds and $^3CDOM^*$, by means of steady-state irradiation experiments. Finally, the yellow lamp was used for selective excitation of Rose Bengal, to produce $^1O_2$.

Bz^- and AcPh were irradiated separately, and initial concentration values in different experiments ranged between 2.5 and 5 μM. The irradiated Bz^- solutions (pH ~ 7) contained the studied compound in the same carboxylate (deprotonated) form in which it would occur in natural waters.

The spectral photon flux density in the solutions subject to irradiation was determined by a combination of lamp spectral measurements (Ocean Optics USB2000 CCD spectrophotometer) and chemical actinometry with 2-nitrobenzaldehyde (Bacilieri et al., 2022). Details are described in Text S1 of the Supplementary Material (hereinafter SM), which also reports the lamp spectra (Fig. S1).

2.3. Instrumental analysis

Absorption spectra were measured with a Varian Cary 100 Scan UV–Vis double-beam spectrophotometer, using Hellma quartz cuvettes (1 cm optical path length).

After scheduled irradiation times, the cells were withdrawn from the lamp and their contents was analysed by liquid chromatography (HPLC-UV). The instrument used was a Merck-Hitachi chromatograph, equipped with AS2000A autosampler (60 μL injection volume), L-6200 and L-6000 pumps for high-pressure binary gradients, and L-4200 UV–Vis detector. The instrument mounted a Merck LiChroCART® 125–4 column, packed with LiChrospher® 100 RP-18 (5 μm). Elution (1 mL min^{-1} flow rate) was carried out with a mixture of 40 % acetonitrile and 60 % water, acidified with H_3PO_4 to pH 3. The combinations of detection wavelengths and retention times were 225 nm and 2.75 min for Bz^-, and 245 nm and 4.60 min for AcPh. The quantification limits for the two compounds were around 0.1 μM. 2-Nitrobenzaldehyde used for actinometry measurements was determined with the same column, eluting (1 mL min^{-1}) with a mixture of 35 % methanol and 65 % acidified water (pH 3, H_3PO_4), with 7.3 min retention time and detection at 258 nm.

2.4. Laser flash photolysis experiments

The fourth harmonic (266 nm) of a Quanta Ray GCR 130–01 Nd:YAG laser system was used to generate and follow the reactivity of $Br_2^{\bullet-}$ in aqueous solution, in the presence of Bz^- and AcPh. The excitation energy was 36 mJ/pulse and an individual cuvette sample (3 mL volume) was used for a maximum of four consecutive laser shots. The spectroscopic system has been described before (Brigante et al., 2014).

$Br_2^{\bullet-}$ was generated through photolysis of 10 mM H_2O_2 in the presence of 10 mM Br^-. Under such conditions, the presence of a long-lived transient species absorbing from 270 to 550 nm with a maximum at 360 nm ($\varepsilon \sim 9.9 \times 10^3\ M^{-1}\ cm^{-1}$) was assigned to the formation of $Br_2^{\bullet-}$ (Hug, 1981). The second-order reaction rate constants of $Br_2^{\bullet-}$ with Bz^- and AcPh were determined from the slopes of the regression lines of the logarithmic decays of the $Br_2^{\bullet-}$ transient (monitored at 360 nm), as a function of the concentration of each selected aromatic compound (Stern-Volmer method). The error was estimated as ±σ, obtained from the scattering of the experimental data around the linear fit line.

2.5. Environmental fate modelling

Photodegradation kinetics of Bz^- and AcPh were modelled with the APEX software (Aqueous Photochemistry of Environmentally-occurring Xenobiotics) (Vione, 2020). This software predicts pseudo-first order photodegradation rate constants by direct photolysis and indirect photochemistry, as a function of sunlight irradiance, water depth, and water chemistry (concentration values of photochemically relevant compounds: nitrate, nitrite, bicarbonate, carbonate, and dissolved organic carbon, DOC) (Silva et al., 2015; Silva et al., 2019; Vione, 2020). APEX assumes well-mixed water bodies under clear-sky conditions, and in these circumstances it has been shown to predict environmental photodegradation kinetics with good accuracy (Avetta et al., 2016).

The volatilisation rate constant of AcPh from aqueous environments was predicted with the EPISUITE™ package by US-EPA (US-EPA, 2021), based on molecular structure (quantitative structure-activity relationship). Water depth was varied in the range of 1 to 5 m, while it was assumed 1 m s^{-1} wind speed. EPISUITE™ (AOPWIN sub-package) was also used for the prediction of the reaction rate constant between AcPh and gas-phase $^{\bullet}OH$, assuming average $[^{\bullet}OH_{(g)}] = 1.5 \times 10^6\ cm^{-3}$.

3. Results and discussion

To assess the photochemical degradation potential of Bz^- and AcPh, all the reaction rate constants with photochemically produced reactive intermediates (PPRIs) and the direct photolysis quantum yields need to be retrieved from literature, or measured through laboratory experiments.

The second-order reaction rate constants of Bz^- and AcPh with $^{\bullet}OH$ are known from the literature, and they are both equal to $5.9 \times 10^9\ M^{-1}\ s^{-1}$ (Buxton et al., 1988; Wols and Hofman-Caris, 2012). Furthermore, Bz^- is known not to react with $CO_3^{\bullet-}$ to a significant extent (Vione et al., 2010; Wojnárovits et al., 2020), while AcPh has a kinetic constant with $CO_3^{\bullet-}$ of $k_{AcPh,CO3^{\bullet-}} = 1 \times 10^7\ M^{-1}\ s^{-1}$ (Neta et al., 1988) (see Table S1 in SM for a rate constant summary).

Irradiation experiments, carried out in the framework of this work, allowed for excluding significant reactions of the studied compounds with either ^{3}CBBP* (and, therefore, ^{3}CDOM*) or $^1O_2$ (see Figs. S2, S3 in SM). Note that CBBP was here used as CDOM proxy, and the reduction potential of ^{3}CBBP* (1.8 V) is included in the typical range of ^{3}CDOM* reduction potentials (1.5–1.9 V; McNeill and Canonica, 2016; Minella et al., 2018). Therefore, it is unlikely that naturally-occurring ^{3}CDOM* are able to trigger significant degradation of either Bz^- or AcPh.

Differently from Bz^-, AcPh was found to undergo direct photolysis to a significant extent under the UVB lamp. UVB irradiation of 5 μM AcPh (pH 7, phosphate buffer) produced degradation with pseudo-first order kinetics, and initial degradation rate $R_{AcPh} = (4.94 \pm 1.02) \times 10^{-12}\ M\ s^{-1}$. In contrast, no AcPh degradation was observed in the dark. The UVB photon flux absorbed by AcPh (Braslavsky, 2007) was determined as $P_{a,AcPh} = \int_\lambda p^\circ(\lambda)[1 - 10^{-\varepsilon_{AcPh}(\lambda)\ b\ C_{AcPh}}]d\lambda = 5.3 \times 10^{-8}$ Einstein $L^{-1}\ s^{-1}$, where $p^\circ(\lambda)$ is the spectral photon flux density (measured by chemical actinometry) that passes through the irradiated solutions at the wavelength λ (Fig. S1, SM), $\varepsilon_{AcPh}(\lambda)$ the molar absorption coefficient of AcPh (Fig. S1, SM), $b = 0.4$ cm the optical path length of the irradiated solutions, and $C_{AcPh} = 5$ μM. The direct photolysis quantum yield of AcPh was calculated as $\Phi_{AcPh} = R_{AcPh}\ (P_{a,AcPh})^{-1} = (9.2 \pm 1.9) \times 10^{-5}$ mol Einstein^{-1}. By comparison, Bz^- did not undergo direct photolysis to a significant extent under the same irradiation conditions. However, Bz^- has been shown to undergo direct photolysis under UVC irradiation, with a quantum yield of 6×10^{-2} mol Einstein^{-1} (Oussi et al., 1998).

3.1. Photochemical persistence of Bz^- and AcPh in natural surface waters

Based on the above photoreaction parameters, the photochemical degradation kinetics of Bz^- and AcPh in sunlit natural waters were assessed by means of the APEX software (see Fig. 1). The assumed conditions of sunlight irradiation ('day') correspond to the 24-h-round spring equinox at 45°N latitude. As such, they also represent approximate year averages at mid latitude under fair-weather conditions (Vione, 2020). The selected concentrations of NO_3^-, NO_2^-, HCO_3^-, and CO_3^{2-} are reasonable values for surface waters (Minero et al., 2007).

Calculation results suggest that AcPh direct photolysis would play minor role, thus Bz^- would be photodegraded by $^{\bullet}OH$ only, while AcPh would react with both $^{\bullet}OH$ and $CO_3^{\bullet-}$. Predicted photodegradation lifetimes range from 1 to 2 weeks to several months. This result looks reasonable, when considering that there is for instance experimental evidence that Bz^- is mainly degraded by $^{\bullet}OH$ in irradiated natural water samples, where it would persist for at least some weeks (Sun, 2015).

Photodegradation kinetics would be highly dependent on the environmental conditions. Kinetics would be the fastest in shallow waters with low DOC, because: *(i)* shallow waters are better illuminated by sunlight than deep waters (Loiselle et al., 2008), the bottom layer of which is usually

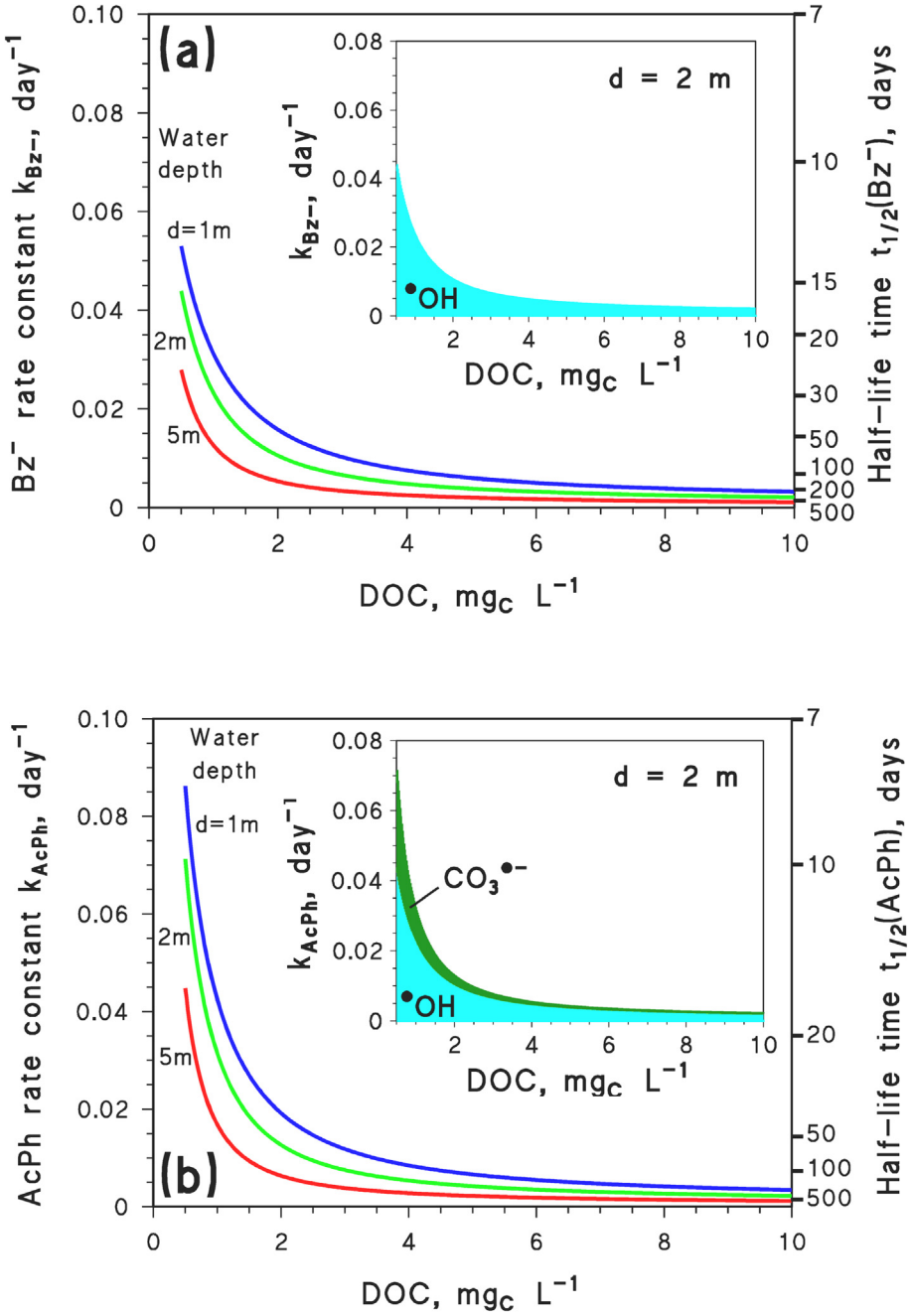

Fig. 1. Modelled first-order phototransformation rate constants (k, left Y-axis) and corresponding half-life times ($t_{1/2} = \ln 2\, k^{-1}$; right Y-axis) as a function of the DOC, for different values of the water depth d: (a) Bz^-; (b) AcPh. Other water parameters: 10^{-4} M NO_3^-, 10^{-6} M NO_2^-, 10^{-3} M HCO_3^-, and 10^{-5} M CO_3^{2-}. The relative importance of the different photoreaction pathways is shown as figure inserts (2 m depth). The phototransformation of Bz^- is predicted to take place by reaction with $^{\bullet}OH$ only. The assumed 'day' corresponds to the spring equinox at 45°N latitude, under fair-weather conditions.

in the dark, and *(ii)* organic matter is a major scavenger of both $^{\bullet}OH$ and $CO_3^{\bullet-}$ (Yan et al., 2019) and it acts as a light-screening agent, which inhibits the direct photolysis of other compounds including the photosensitisers nitrate and nitrite.

Therefore, kinetics of photodegradation by $^{\bullet}OH$ and $CO_3^{\bullet-}$ are slower at high DOC values. In this framework, the absorbance of natural water was simulated as $A_w = 45\, d\, \mathrm{DOC}\, e^{-0.015\,\lambda}$, where A_w is unitless and d is the water depth in metres (Vione, 2020).

The important role played by $^{\bullet}OH$ and/or $CO_3^{\bullet-}$ in the photodegradation of Bz^- and AcPh suggests that nitrate concentration might affect phototransformation kinetics considerably. Nitrate is in fact a direct $^{\bullet}OH$ and indirect $CO_3^{\bullet-}$ source (Vione and Scozzaro, 2019) and, as shown in Fig. S4 (SM), the pseudo-first order transformation rate constants of both Bz^- and AcPh increase with increasing nitrate, all other conditions being equal.

The nitrate effect is substantial at low DOC (increase by 4–5 times in degradation kinetics when passing from 10^{-6} M to 10^{-4} M NO_3^-, for DOC = 1 $mg_C\, L^{-1}$; Fig. S4 in SM), while the effect is much less important at higher DOC values. The rationale is that high DOC entails the scavenging by DOM of the vast majority of $^{\bullet}OH$ and $CO_3^{\bullet-}$ photogenerated by nitrate. CDOM is another significant $^{\bullet}OH$ source, especially at high DOC, but in the presence of elevated DOC values a large fraction of $^{\bullet}OH$ photogenerated by CDOM would be scavenged by DOM.

3.2. Possible environmental scenarios

Different scenarios of photoinduced degradation in the environment were taken into account for the studied compounds. In the case of non-volatile Bz^- we have considered photodegradation in surface waters only. Bz^- formation kinetics from polystyrene exposed to sunlight have been studied previously (Bianco et al., 2020) and the available data allow for describing a possible scenario where polystyrene degradation yields Bz^-, which is then photodegraded by $^{\bullet}OH$. By so doing, it is possible to assess a potential for Bz^- accumulation in natural waters. In the case of semivolatile AcPh, we simulated a scenario of degradation in both surface waters and the atmosphere, combined with AcPh volatilisation from the aqueous phase to the gas phase.

3.2.1. Benzoate (Bz^-)

In the case of Bz^-, formation kinetics from 0.2 % v/v polystyrene in water under environmental irradiation is known (Bianco et al., 2020), which would be representative of strong water pollution by polystyrene particles. The scenario considered here assumes that polystyrene particles occur near the water surface (*i.e.*, they float), while released Bz^- undergoes diffusion in the whole water volume. In addition, it is assumed that Bz^- is degraded by reaction with $^{\bullet}OH$ (see Fig. 1a), following first-order kinetics. Details of kinetic calculations are provided in Text S2 of SM. The time trend of Bz^- that results from the formation-photodegradation budget is the following:

$$[Bz^-] = \frac{R_{Bz-}\, d_o}{k_{Bz-}\, d}\left(1 - e^{-k_{Bz-}t}\right) \quad (1)$$

where $R_{Bz-} = 3.1 \times 10^{-7}$ M day^{-1} and $d_o = 0.023$ m are derived from the literature (Bianco et al., 2020). They are, respectively, the experimental formation rate of Bz^- from polystyrene under real sunlight and the experimental water depth, see also Text S2 in SM. Furthermore, d [m] is the assumed depth of the water body, k_{Bz-} [day^{-1}] the pseudo-first order degradation rate constant of Bz^- (modelled with APEX), and t is time in days.

To simplify calculations, as an approximation we kept k_{Bz-} constant with time at its equinox value (yearly average). In other words, the value of k_{Bz-} we used varied in different conditions of, *e.g.*, water depth (d) and DOC as per Fig. 1a, but its seasonal fluctuations were neglected. Seasonal variations were neglected also in the case of R_{Bz-}, which is a year average as well. Considering that polystyrene releases Bz^- under irradiation and that Bz^- would react with photogenerated $^{\bullet}OH$, it is likely that R_{Bz-} and k_{Bz-} vary in parallel and that their seasonal variations cancel out at least partially in Eq. (1). With these approximations, the Bz^- time trends in different conditions are shown in Fig. 2.

Eq. (1) predicts that [Bz^-] reaches a plateau after quite long time (high t values). The plateau concentration of Bz^- results from the budget between generation from polystyrene and degradation by $^{\bullet}OH$. Furthermore, the initial increase in [Bz^-] (low t values, $t < 50$ days) mostly depends on water depth d: if water is deep, generated Bz^- is diluted in a higher volume, and its concentration increase is slower (and *vice versa*, in the case of shallow water). At later times, water depth has two opposite impacts on the Bz^- time trend, which partially offset each other (Text S2 in SM): the former is the dilution effect, already mentioned; the latter is the fact that the deeper is water, the slower is Bz^- degradation upon reaction with $^{\bullet}OH$ (see Fig. 1a).

The plateau concentration of Bz^- strongly depends on the DOC: if DOC is high, Bz^- degradation is slow and [Bz^-] can reach higher values with potential accumulation; the opposite happens at low DOC.

As shown in Fig. 2, Bz^- would eventually reach sub-μM levels. By comparison, in the literature experiment that yielded $R_{Bz-} = 3.1 \times 10^{-7}$ M day^{-1} (Bianco et al., 2020) the volume was quite small ($d = 0.023$ m, thereby ensuring limited dilution) and the aqueous phase did not contain $^{\bullet}OH$ sources. In such circumstances, Bz^- could accumulate with little dilution or degradation and reach 0.13 mM levels in 14 months. In the current simulations, for water depths of some metres and in the presence of Bz^- degradation by $^{\bullet}OH$, we predict [Bz^-] to reach values that are lower by 2–3 orders of magnitude (sub-μM *vs.* sub-mM), which looks reasonable.

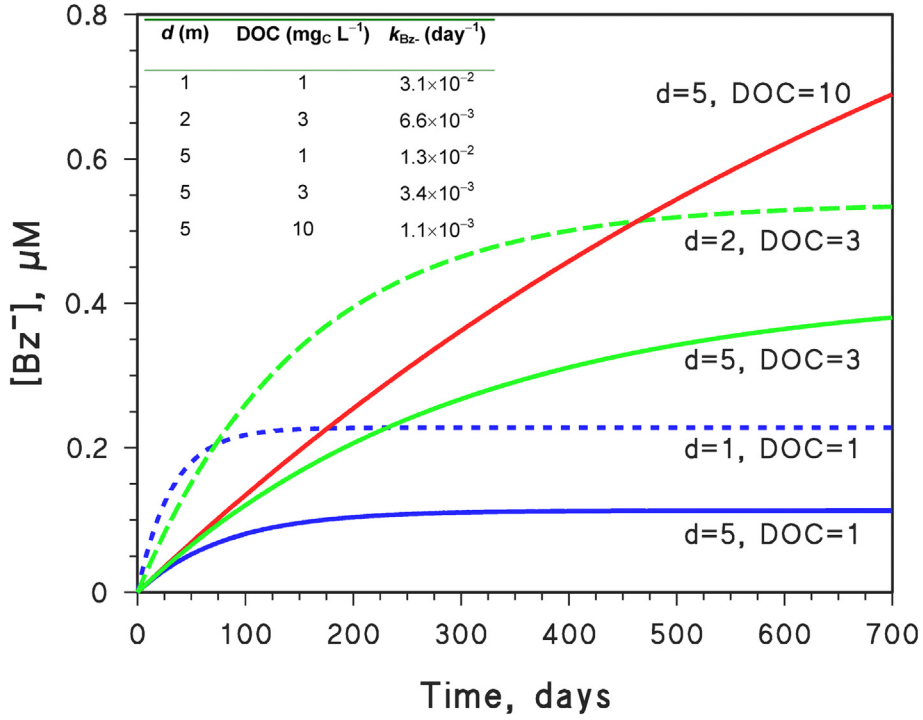

Fig. 2. Time trends of Bz^- in different surface-water scenarios, as predicted by Eq. (1). The value of k_{Bz-} in each condition (see the table insert) was referred to clear-sky spring equinox (approximate year average). The measure unit of the DOC value reported near each curve is [$mg_C\ L^{-1}$], that of d (water depth) is [m]. Other water conditions for the APEX modelling of k_{Bz-} are as follows: 10^{-4} M NO_3^-, 10^{-6} M NO_2^-, 10^{-3} M HCO_3^-, and 10^{-5} M CO_3^{2-}.

3.2.2. Acetophenone (AcPh)

As mentioned before, AcPh could be degraded in water by (mainly) $^{\bullet}OH$ and $CO_3^{\bullet-}$, or volatilise to the gas phase where it would react with $^{\bullet}OH_{(g)}$, similarly to other semivolatile compounds (Arsene et al., 2022). The overall scenario is depicted in Scheme 1a, and two specific scenarios are illustrated in Scheme 1b.

Starting from AcPh in water ($AcPh_w$) at initial concentration C_o, the kinetic system depicted in Scheme 1 gives the time trends for [$AcPh_w$] and [$AcPh_g$] (w = water phase, g = gas phase) described by Eqs. (2), (3), which are solutions of differential equations and were derived in similar way as Arsene et al. (2022) (see Scheme 1 for the meaning of the different parameters):

$$[AcPh_w] = C_o\, e^{-(k_{AcPh}+k_v)\,t} \tag{2}$$

$$[AcPh_g] = \frac{k_v\, C_o}{k_g - k_{AcPh} - k_v}\left[e^{-(k_{AcPh}+k_v)\,t} - e^{-k_g t}\right] \tag{3}$$

The values of k_{AcPh} as a function of water depth and DOC were modelled with APEX (see Fig. 1b); k_g was assessed as 0.12 day^{-1} by EpiSuite 4.1 (AOPWIN), assuming average [$^{\bullet}OH_{(g)}$] = 1.5 × 10^6 cm^{-3} (Lelieveld et al., 2016); finally, the estimated value of k_v (0.016–0.087 day^{-1}; EpiSuite 4.1) depends on water depth and is lower as d is higher ($1 < d < 5$ m, see Fig. S6 in SM).

The time trends of [$AcPh_w$] and [$AcPh_g$], obtained according to Eqs. (2) and (3), are shown in Fig. 3 for different values of the water depth d (1 or 5 m) and of the DOC (1, 3, or 10 $mg_C\ L^{-1}$). A first issue is that volatilisation would usually play the main role in the removal of AcPh from the aqueous phase, except for d = 5 m and DOC = 1 $mg_C\ L^{-1}$ where volatilisation and photodegradation would be comparable (Scheme 1b). Because of the important weight of k_v in Eq. (2), the DOC value (which only affects k_{AcPh}) would have relatively limited effect on the time trend of [$AcPh_w$] (Fig. 3a,c). Furthermore, removal kinetics of AcPh from the aqueous phase would be considerably faster at d = 1 m (where k_{AcPh} and especially k_v are considerably higher, see Fig. 3a and Scheme 1b) than at d = 5 m (Fig. 3c).

The initial increase of [$AcPh_g$] is controlled by k_v and, therefore, it does not depend on the DOC (Fig. 3b,d). The gas-phase degradation of AcPh is also DOC-independent, because k_g = 0.12 day^{-1} is only linked to the value of [$^{\bullet}OH_{(g)}$]. In spite of these issues, there are some differences in the [$AcPh_g$] time trends (Fig. 3b,d) that depend on the DOC value of the aqueous phase. The reason is that low DOC entails slightly faster decay of $AcPh_w$ (Fig. 3a,c), because of higher values of [$^{\bullet}OH$] and [$CO_3^{\bullet-}$] in the aqueous phase that lead to higher k_{AcPh}. As $AcPh_w$ undergoes slightly faster consumption at low DOC, a lesser amount is available for partitioning to the gas phase and, therefore, $AcPh_g$ reaches slightly lower concentration values if the water DOC is low (Fig. 3b,d).

Overall, model results suggest that volatilisation and reaction with gas-phase $^{\bullet}OH$ have potential to play key roles in the environmental fate of AcPh.

3.3. Reactivity with $Br_2^{\bullet-}$, and implications for photodegradation in seawater

The radicals $^{\bullet}OH$ and $CO_3^{\bullet-}$ are expected to play important roles in the photodegradation of Bz^- (only $^{\bullet}OH$) and AcPh (both species) in sunlit

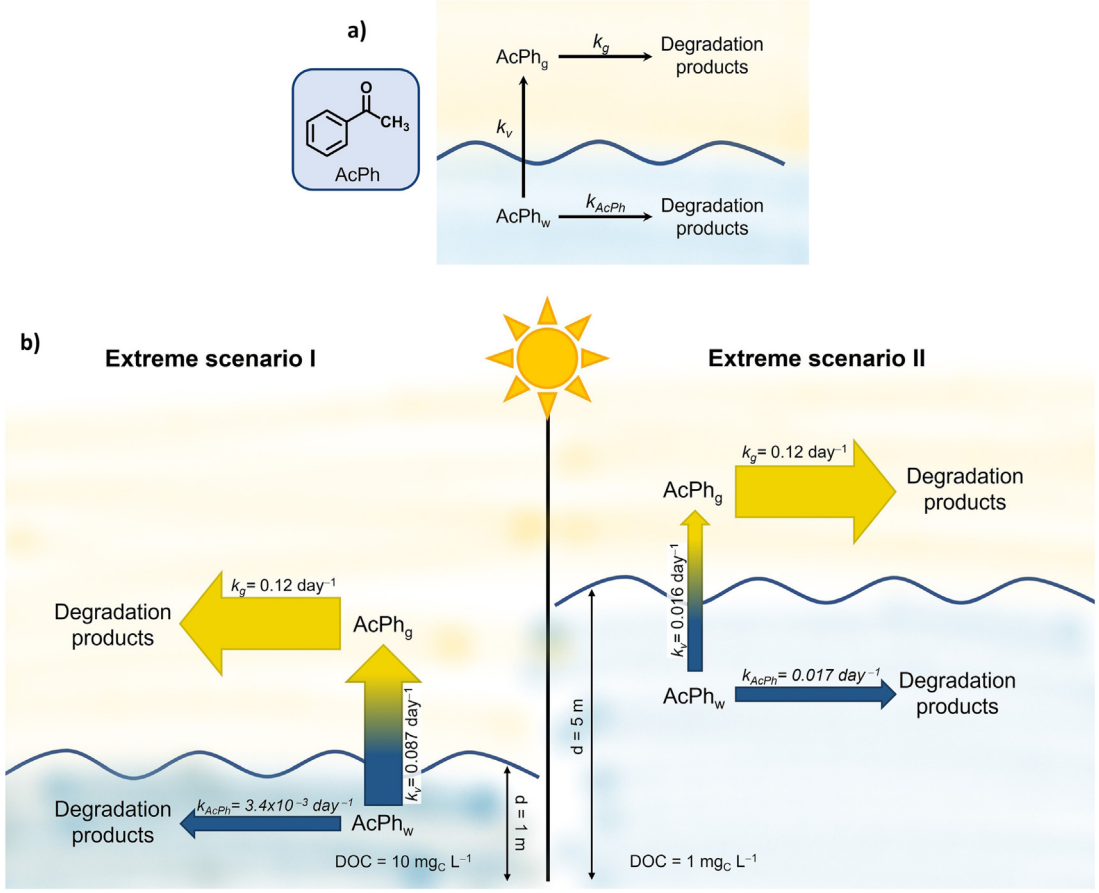

Scheme 1. In a) overall reaction scheme of AcPh in the aqueous phase (w) and in the gas phase (g). The pseudo-first order AcPh rate constants are also shown: k_{AcPh} is the photodegradation rate constant in water, modelled with APEX; k_v is the volatilisation rate constant, modelled with EpiSuite 4.1; k_g is the degradation rate constant upon reaction with $^{\bullet}OH_{(g)}$, also modelled with EpiSuite 4.1 (AOPWIN). In b) are represented two extreme scenarios: scenario I is characterised by water depth d = 1 m and DOC = 10 $mg_C\ L^{-1}$, scenario II assumes d = 5 m and DOC = 1 $mg_C\ L^{-1}$. The arrow sizes are roughly proportional to the rate constant values.

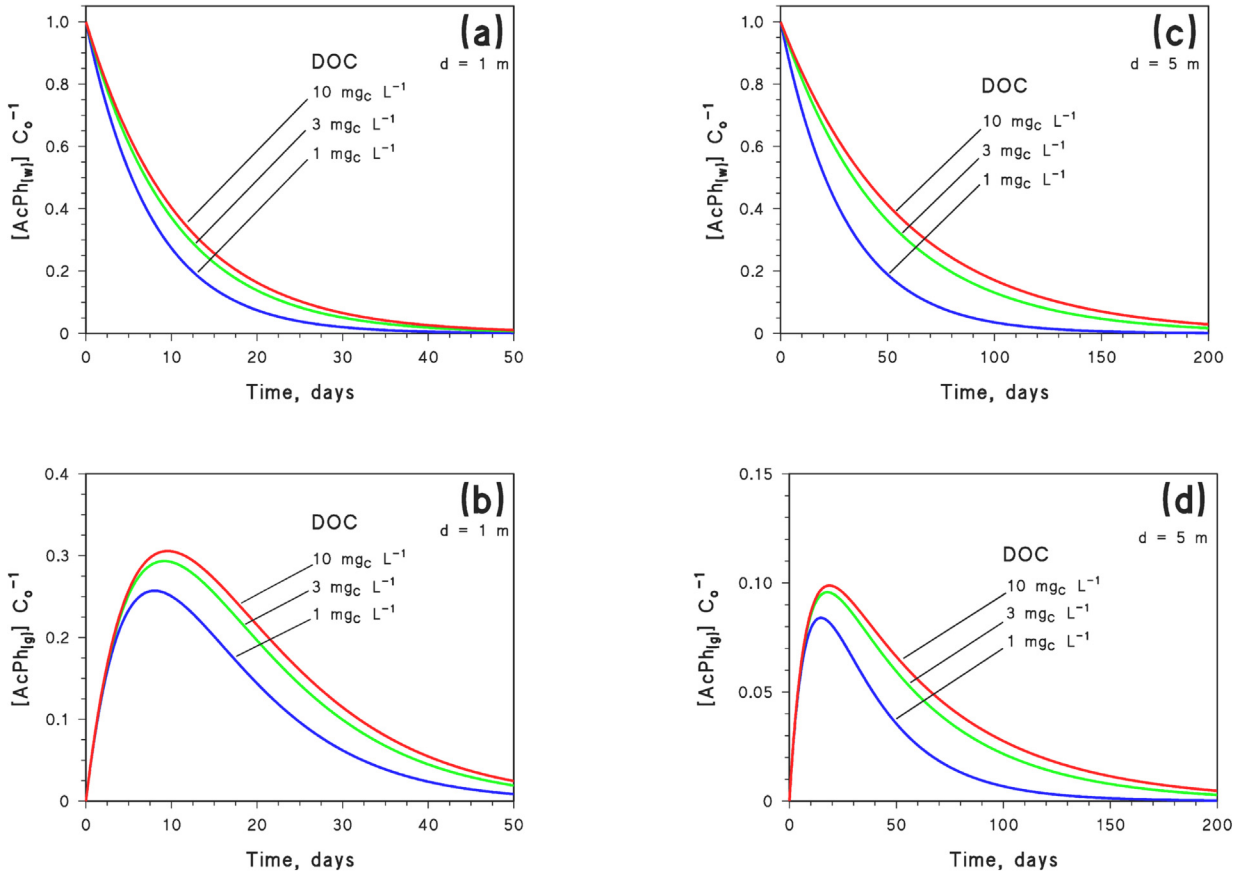

Fig. 3. Modelled time trends of $[AcPh_w]$ ((a,c), Eq. (2)) and $[AcPh_g]$ ((b,d), Eq. (3)), for different values of the DOC and for water depth d = 1 m (a,b) and 5 m (c,d). Other water conditions: 10^{-4} M NO_3^-, 10^{-6} M NO_2^-, 10^{-3} M HCO_3^-, and 10^{-5} M CO_3^{2-}. 'Day' = fair-weather spring equinox at 45°N.

freshwaters. However, in the case of brackish waters and saltwater, $^{\bullet}OH$ would be very effectively scavenged by bromide (Buxton et al., 1988; Parker and Mitch, 2016). This phenomenon would strongly inhibit the $^{\bullet}OH$-mediated processes, and it would also block the main $CO_3^{\bullet-}$ formation pathway (HCO_3^-/CO_3^{2-} oxidation by $^{\bullet}OH$ itself; Canonica et al., 2005). At the same time, the reactive radical $Br_2^{\bullet-}$ would be generated by $^{\bullet}OH$ in the

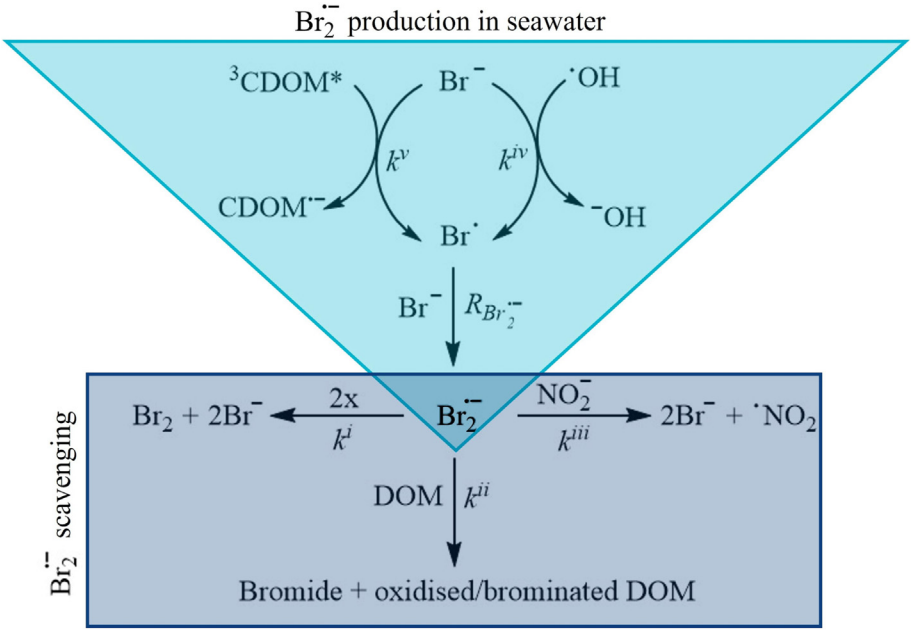

Scheme 2. Main reactions accounting for the production (in the light blue triangle) and scavenging/quenching (in the dark blue rectangle) of $Br_2^{\bullet-}$ in bromide-containing natural waters. The relevant rate constants are those used in Eqs. (4), (5): $k^i = 2 \times 10^9$ M^{-1} s^{-1}, $k^{ii} = 306$ L mg_C^{-1} s^{-1}, $k^{iii} = 2 \times 10^7$ M^{-1} s^{-1}, $k^{iv} = 1.1 \times 10^{10}$ M^{-1} s^{-1}, and $k^v = 3 \times 10^9$ M^{-1} s^{-1} (see De Laurentiis et al., 2012).

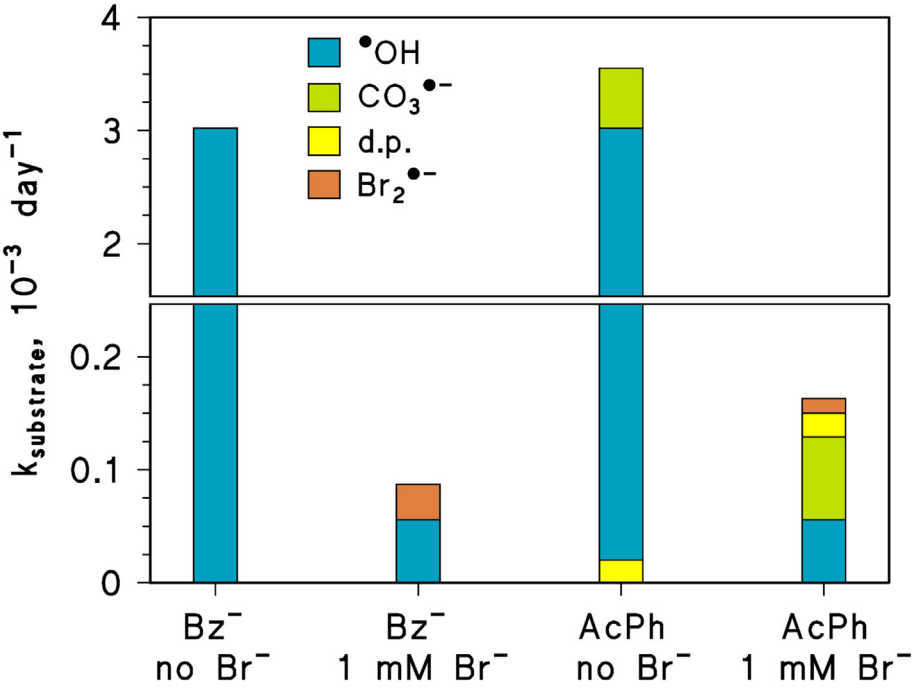

Fig. 4. Modelled pseudo-first order photodegradation rate constants of Bz^- and AcPh, in the absence of bromide and in the presence of 1 mM bromide. The colour code highlights the different photoreaction pathways: hydroxyl ($^{\bullet}OH$) and carbonate ($CO_3^{\bullet-}$) radicals, dibromide radical anions ($Br_2^{\bullet-}$), and direct photolysis (d.p.). APEX was used to calculate reaction kinetics by $^{\bullet}OH$, $CO_3^{\bullet-}$, and the direct photolysis in all conditions, and to assess [$^{\bullet}OH$] and [^{3}CDOM*] for the calculation of $R_{Br_2^{\bullet-}}$ and [$Br_2^{\bullet-}$] (Eqs. (4), (5)). Other conditions (relevant to coastal seawater; Chen, 2001): 5 m depth, 3.5 $mg_C\ L^{-1}$ DOC, 10^{-5} M NO_3^-, 10^{-7} M NO_2^-, 2.5 × 10^{-3} M HCO_3^-, and 2.5 × 10^{-5} M CO_3^{2-}. The assumed 'day' corresponds to the spring equinox at 45°N latitude, under fair-weather conditions. Note the break in the Y-axis.

presence of bromide (Parker and Mitch, 2016): the main processes connected with the occurrence of $Br_2^{\bullet-}$ in environmental waters are depicted in Scheme 2.

Based on Scheme 2, and applying the steady-state approximation to both $Br^{\bullet}$ and $Br_2^{\bullet-}$, one gets the following equations for, respectively, $Br_2^{\bullet-}$ formation rate and its steady-state concentration (De Laurentiis et al., 2012):

$$R_{Br_2^{\bullet-}} = [Br^-]\left(k^{iv}[^{\bullet}OH] + k^{v}[^3CDOM^*]\right) \quad (4)$$

$$[Br_2^{\bullet-}] = \frac{-\left(k^{ii}DOC + k^{iii}[NO_2^-]\right) + \sqrt{\left(k^{ii}DOC + k^{iii}[NO_2^-]\right)^2 + 4k^i R_{Br_2^{\bullet-}}}}{2k^i} \quad (5)$$

where the reaction rate constants k^i-k^v are those shown in Scheme 2.

$Br_2^{\bullet-}$ is quite reactive and might have a role in degradation reactions. Therefore, it is very interesting to assess the reactivity of the studied compounds with $Br_2^{\bullet-}$. Laser flash photolysis experiments (see Fig. S7 in SM) yielded $k_{Bz^-,\ Br_2^{\bullet-}} = (4.8 \pm 0.5) \times 10^7\ M^{-1}\ s^{-1}$ and $k_{AcPh,\ Br_2^{\bullet-}} = (2.0 \pm 0.5) \times 10^7\ M^{-1}\ s^{-1}$ as the second-order reaction rate constants of $Br_2^{\bullet-}$ with, respectively, Bz^- and AcPh.

On the basis of the $Br_2^{\bullet-}$ second-order reaction rate constants obtained by laser flash photolysis ($k_{Substrate,\ Br_2^{\bullet-}}$), it is possible to assess the first-order rate constants of degradation by $Br_2^{\bullet-}$ as $k_{Substrate} = k_{Substrate,\ Br_2^{\bullet-}} \times [Br_2^{\bullet-}]$, where 'Substrate' = Bz^- or AcPh. The effect of bromide on the overall kinetics (pseudo-first order rate constants) and on the different pathways of Bz^- and AcPh degradation is shown in Fig. 4.

First of all, 1 mM bromide (relevant to seawater conditions; Fukushi et al., 2000) would slow down photodegradation of both Bz^- and AcPh by over ten times. The $^{\bullet}OH$ pathway would be particularly affected due to $^{\bullet}OH$ scavenging by Br^-, followed by $CO_3^{\bullet-}$ that would also be inhibited considerably. Although both Bz^- and AcPh would be degraded by $Br_2^{\bullet-}$ to a significant extent in the presence of 1 mM Br^-, this process would be unable to offset inhibition of the $^{\bullet}OH$ and $CO_3^{\bullet-}$ pathways. Therefore, Bz^- and AcPh are potentially more photostable in saline waters than in freshwater.

4. Conclusions

The experimental data obtained in this work allowed for excluding that direct photolysis or reactions with $^1O_2$ or ^{3}CDOM* could play significant role in the environmental fate of Bz^- and AcPh in sunlit freshwaters. In contrast, photochemical modelling showed that $^{\bullet}OH$ would contribute to the environmental attenuation of Bz^-, while $^{\bullet}OH$ and $CO_3^{\bullet-}$ would take part in the transformation of AcPh. Such photoreaction pathways would be enhanced in the presence of low DOC or high nitrate levels, while high DOC would protect the studied compounds from photodegradation. High nitrate, which enhances photodegradation of both Bz^- and AcPh, is relevant to plastic pollution because the spreading of fertilizers (of which nitrate is an important component) plays major role in the occurrence of microplastics in surface waters (Kumar et al., 2020).

Differently from Bz^-, AcPh is volatile enough to undergo phase transfer from surface waters to the atmosphere, where it would react with gas-phase $^{\bullet}OH$. Such a process could be highly competitive with the aqueous-phase photodegradation of AcPh by $^{\bullet}OH$ and $CO_3^{\bullet-}$. Finally, although there is potential for $Br_2^{\bullet-}$ to play significant role in the photodegradation of both Bz^- and AcPh at seawater bromide levels, the scavenging of $^{\bullet}OH$ by bromide would slow down considerably photodegradation kinetics of both Bz^- and AcPh. Therefore, Bz^- and AcPh photodegradation should be much slower in seawater compared to freshwaters.

CRediT authorship contribution statement

Debora Fabbri: Investigation, Validation, Formal analysis, Data curation, Writing – original draft. **Luca Carena:** Investigation, Formal analysis, Data curation, Writing – original draft, Writing – review & editing. **Debora Bertone:** Investigation, Data curation, Writing – original draft. **Marcello Brigante:** Investigation, Validation, Data curation, Writing – review & editing. **Monica Passananti:** Funding acquisition, Conceptualization, Writing – review & editing. **Davide Vione:** Conceptualization, Investigation, Supervision, Validation, Data curation, Writing – original draft, Writing – review & editing.

Data availability

Data will be made available on request.

Declaration of competing interest

The authors declare that they have no known competing financial interests or personal relationships that could have appeared to influence the work reported in this paper.

Acknowledgements

This work is part of a project that has received funding from the European Research Council (ERC) under the European Union's Horizon 2020 research and innovation program, grant agreement No 948666 – ERC-2020-StG NaPuE, from Fondazione CRT Erogazioni Ordinarie 2020 n. 2020.1874, and from MIUR Call FARE project NATtA n. R20T85832Z.

Appendix A. Supplementary data

Further experimental results, chemical actinometry, rate constants summary, detailed description of the polystyrene-benzoate photochemical scenario. Supplementary data to this article (SM) can be found online at https://doi.org/10.1016/j.scitotenv.2023.162729.

References

Andrady, A.L., Barnes, P.W., Bornman, J.F., Gouin, T., Madronich, S., White, C.C., Zepp, R.G., Jansen, M.A.K., 2022. Oxidation and fragmentation of plastics in a changing environment; from UV-radiation to biological degradation. Sci. Total Environ. 851 (2), 158022.

Arsene, C., Bejan, I.G., Roman, C., Olariu, R.I., Minella, M., Passananti, M., Carena, L., Vione, D., 2022. Evaluation of the environmental fate of a semivolatile transformation product of ibuprofen based on a simple two-media fate model. Environ. Sci. Technol. 56, 15650–15660.

Avetta, P., Fabbri, D., Minella, M., Brigante, M., Maurino, V., Minero, C., Pazzi, M., Vione, D., 2016. Assessing the phototransformation of diclofenac, clofibric acid and naproxen in surface waters: model predictions and comparison with field data. Water Res. 105, 383–394.

Bacilieri, F., Vähätalo, A.V., Carena, L., Wang, M., Gao, P., Minella, M., Vione, D., 2022. Wavelength trends of photoproduction of reactive transient species by chromophoric dissolved organic matter (CDOM), under steady-state polychromatic irradiation. Chemosphere 306, 135502.

Bianco, A., Sordello, F., Ehn, M., Vione, D., Passananti, M., 2020. Degradation of nanoplastics in the environment: reactivity and impact on atmospheric and surface waters. Sci. Total Environ. 742, 140413.

Braslavsky, S.E., 2007. Glossary of terms used in photochemistry. Pure Appl. Chem. 79, 293–465.

Brigante, M., Minella, M., Mailhot, G., Maurino, V., Minero, C., Vione, D., 2014. Formation and reactivity of the dichloride radical ($Cl_2^{\bullet-}$) in surface waters: a modelling approach. Chemosphere 95, 464–469.

Burgos-Aceves, M.A., Abo-Al-Ela, H.G., Faggio, C., 2021. Physiological and metabolic approach of plastic additive effects: immune cells responses. J. Hazard. Mater. 404 (A), 124114.

Buxton, G.V., Greenstock, C.L., Helman, P.W., Ross, A.B., 1988. Critical review of rate constants for reactions of hydrated electrons, hydrogen atoms and hydroxyl radicals ($^{\bullet}OH/^{\bullet}O^-$) in aqueous solution. J. Phys. Chem. Ref. Data 17, 513–886.

Canonica, S., Kohn, T., Mac, M., Real, F.J., Wirz, J., Von Gunten, U., 2005. Photosensitizer method to determine rate constants for the reaction of carbonate radical with organic compounds. Environ. Sci. Technol. 39, 9182–9188.

Carena, L., Puscasu, C.G., Comis, S., Sarakha, M., Vione, D., 2019. Environmental photodegradation of emerging contaminants: a re-examination of the importance of triplet-sensitised processes, based on the use of 4-carboxybenzophenone as proxy for the chromophoric dissolved organic matter. Chemosphere 237, 124476.

Chen, C.T.A., 2001. General chemistry of seawater. Oceanography. Vol. I. UNESCO-EOLSS, pp. 1–26.

De Laurentiis, E., Minella, M., Maurino, V., Minero, C., Mailhot, G., Sarakha, M., Brigante, M., Vione, D., 2012. Assessing the occurrence of the dibromide radical ($Br_2^{\bullet-}$) in natural waters: measures of triplet-sensitised formation, reactivity, and modelling. Sci. Total Environ. 439, 299–306 2012 Nov 15.

Ding, R., Ouyang, Z., Bai, L., Zuo, X., Xiao, C., Guo, X., 2022. What are the drivers of tetracycline photolysis induced by polystyrene microplastic? Chem. Eng. J. 435, 134827.

Frias, J., Nash, R., 2019. Microplastics: finding a consensus on the definition. Mar. Pollut. Bull. 138, 145–147.

Fukushi, K., Ishio, N., Urayama, H., Takeda, S., Wakida, S., Hiiro, K., 2000. Simultaneous determination of bromide, nitrite and nitrate ions in seawater by capillary zone electrophoresis using artificial seawater as the carrier solution. Electrophoresis 21, 388–395.

Gewert, B., Plassmann, M.M., MacLeod, M., 2015. Pathways for degradation of plastic polymers floating in the marine environment. Environ. Sci. Process. Impacts 17, 1513–1521.

Geyer, R., Jambeck, J.R., Law, K.L., 2017. Production, use, and fate of all plastics ever made. Sci. Adv. 3, 1700782.

Gligorovski, S., Strekowski, R., Barbati, S., Vione, D., 2015. Environmental implications of hydroxyl radicals (•OH). Chem. Rev. 115, 13051–13092.

Guo, Z., Kodikara, D., Shofi Albi, L., Hatano, Y., Chen, G., Yoshimura, C., Wang, J., 2023. Photodegradation of organic micropollutants in aquatic environment: importance, factors and processes. Water 231, 118236.

Hug, G.L., 1981. Optical Spectra of Non-metallic Inorganic Transient Species in Aqueous Solution. NSRDS-NBS 69, US. Government Printing Office, Washington DC.

Jakubowicz, I., Enebro, J., Yarahmadi, N., 2021. Challenges in the search for nanoplastics in the environment - a critical review from the polymer science perspective. Polym. Test. 93, 106953.

Jambeck, J.R., Geyer, R., Wilcox, C., Siegler, T.R., Perryman, M., Andrady, A., Narayan, R., Law, K.L., 2015. Marine pollution. Plastic waste inputs from land into the ocean. Science 347, 768–771.

Katagi, T., 2018. Direct photolysis mechanism of pesticides in water. J. Pestic. Sci. 43, 57–72.

Kumar, M., Xiong, X., He, M., Tsang, D.C.W., Gupta, J., Khan, E., Harrad, S., Hou, D., Ok, Y.S., Bolan, N.S., 2020. Microplastics as pollutants in agricultural soils. Environ. Pollut. 265, 114980.

Lelieveld, J., Gromov, S., Pozzer, A., Taraborrelli, D., 2016. Global tropospheric hydroxyl distribution, budget and reactivity. Atmos. Chem. Phys. 16, 12477–12493.

Liu, L., Xu, K., Zhang, B., Ye, Y., Zhang, Q., Jiang, W., 2021. Cellular internalization and release of polystyrene microplastics and nanoplastics. Sci. Total Environ. 779, 146523.

Loiselle, S.A., Azza, N., Cozar, A., Bracchini, L., Tognazzi, A., Dattilo, A., Rossi, C., 2008. Variability in factors causing light attenuation in Lake Victoria. Freshw. Biol. 53, 535–545.

McNeill, K., Canonica, S., 2016. Triplet state dissolved organic matter in aquatic photochemistry: reaction mechanisms, substrate scope, and photophysical properties. Environ. Sci.: Process.Impacts 18, 1381–1399.

Minella, M., Rapa, L., Carena, L., Pazzi, M., Maurino, V., Minero, C., Brigante, M., Vione, D., 2018. An experimental methodology to measure the reaction rate constants of processes sensitised by the triplet state of 4-carboxybenzophenone as a proxy of the triplet states of chromophoric dissolved organic matter, under steady-state irradiation conditions. Environ. Sci.: Process.Impacts 20, 1007–1019.

Minero, C., Chiron, S., Falletti, G., Maurino, V., Pelizzetti, E., Ajassa, R., Carlotti, M.E., Vione, D., 2007. Photochemical processes involving nitrite in surface water samples. Aquat. Sci. 69, 71–85.

Neta, P., Huie, R.E., Ross, A.B., 1988. Rate constants for reactions of inorganic radicals in aqueous solution. J. Phys. Chem. Ref. Data 17, 1027.

Ossola, R., Jönsson, O.M., Moor, K., McNeill, K., 2021. Singlet oxygen quantum yields in environmental waters. Chem. Rev. 121, 4100–4146.

Oussi, D., Mokrini, A., Chamarro, E., Esplugas, S., 1998. Photodegradation of benzoic acid in aqueous solutions. Environ. Technol. 19, 955–960.

Parker, K.M., Mitch, W.A., 2016. Halogen radicals contribute to photooxidation in coastal and estuarine waters. Proc. Natl. Acad. Sci. U. S. A. 113, 5868–5873.

Rosario-Ortiz, F.L., Canonica, S., 2016. Probe compounds to assess the photochemical activity of dissolved organic matter. Environ. Sci. Technol. 50, 12532–12547.

Salthammer, T., 2022. Microplastics and their additives in the indoor environment. Angew. Chem. Int. Ed. Engl. 61, e202205713.

Schmidt, C., Krauth, T., Wagner, S., 2017. Export of plastic debris by rivers into the sea. Environ. Sci. Technol. 51, 12246–12253.

Silva, M.P., Mostafa, S., McKay, G., Rosario-Ortiz, F.L., Teixeira, A.C.S.C., 2015. Photochemical fate of amicarbazone in aqueous media: laboratory measurement and simulations. Environ. Eng. Sci. 32, 730–740.

Silva, M.P., Acosta, A.M.L., Ishiki, H.M., Rossi, R.C., Mafra, R.C., Teixeira, A.C.S.C., 2019. Environmental photochemical fate and UVC degradation of sodium levothyroxine in aqueous medium. Environ. Sci. Pollut. Res. 26, 4393–4403.

Sun, L., 2015. Study of photochemical formation of hydroxyl radical in natural waters. PhD DissertationChemistry & Biochemistry. Old Dominion University.

US-EPA, 2021. Estimation Programs Interface Suite™ for Microsoft® Windows, v. 4.11. United States Environmental Protection Agency, Washington, DC, USA.

Vione, D., 2020. A critical view of the application of the APEX software (Aqueous Photochemistry of Environmentally-occurring Xenobiotics) to predict photoreaction kinetics in surface freshwaters. Molecules 25, 9.

Vione, D., Scozzaro, A., 2019. Photochemistry of surface fresh waters in the framework of climate change. Environ. Sci. Technol. 53, 7945–7963.

Vione, D., Bagnus, D., Maurino, V., Minero, C., 2010. Quantification of singlet oxygen and hydroxyl radicals upon UV irradiation of surface water. Environ. Chem. Lett. 8, 193–198.

Wojnárovits, L., Tóth, T., Takács, E., 2020. Rate constants of carbonate radical anion reactions with molecules of environmental interest in aqueous solution: a review. Sci. Total Environ. 717, 137219.

Wols, B.A., Hofman-Caris, C.H., 2012. Review of photochemical reaction constants of organic micropollutants required for UV advanced oxidation processes in water. Water Res. 46, 2815–2827.

Yan, S., Song, W., 2014. Photo-transformation of pharmaceutically active compounds in the aqueous environment: a review. Environ. Sci.: Process. Impacts 16, 697–720.

Yan, S., Liu, Y., Lian, L., Li, R., Ma, J., Zhou, H., Song, W., 2019. Photochemical formation of carbonate radical and its reaction with dissolved organic matters. Water Res. 161, 288–296.

Zhu, L., Zhao, S., Bittar, T.B., Stubbins, A., Li, D., 2020. Photochemical dissolution of buoyant microplastics to dissolved organic carbon: rates and microbial impacts. J. Hazard. Mater. 383, 121065.